

Stress Corrosion Cracking Testing in SCW – Results of SSRT Tests

R. Novotny¹, P. Haehner¹, P. Janik¹, J. Siegl², P. Hausild², S. Riplinger¹

¹ Joint Research Center, Institute of Energy, Petten, Netherlands

² Czech Technical University, Prague, Czech Republic

Abstract

The presented paper summarizes the results of stress corrosion cracking (SCC) susceptibility tests in supercritical water (SCW) for austenitic alloys 316L, 316NG, 347HP and Alloy 690 with the aim to identify the maximum applicable SCW temperature and specific failure mechanisms prevailing during slow strain-rate tensile (SSRT) tests in ultra-pure demineralized SCW solution with controlled oxygen content. In addition to the strain rate, which was controlled by the crosshead speed, the oxygen content was varied in the series of tests in the case of austenitic stainless steel 316L. The fractography confirmed that failure was due to a combination of transgranular SCC and transgranular ductile fracture. Based on fractographic findings a phenomenological map describing the SCC regime of SSRT test conditions was proposed for AISI 316L.

Keywords: SCW, SCC, Austenitic Alloys, SSRT, Crack Growth Rate, Pneumatic Bellows

1. Introduction

The European concept of a SCW reactor is a Light Water Reactor (LWR) in the 1000MWe class envisaged to operate above the supercritical pressure ($p > 22.1$ MPa). Inside the reactor core, water at a pressure of 25 MPa is heated from 280 °C to 500 °C [1].

Supercritical water represents an environment with significantly different corrosion properties as compared to liquid water below the critical point. The identification and characterization of candidate alloys for specific reactor components by corrosion, creep and environmentally assisted cracking (EAC) tests at the expected pressures and temperatures is thus one of the most important project tasks.

The coolant leaves the core with an average outlet temperature of 500 °C through the hot steam pipes. This design encompasses considerable differences in coolant properties through the reactor core, most critically, at the low density associated with the reactor core outlet; water is a very aggressive oxidizer and a non-polar solvent, which can dissolve gases like oxygen to complete miscibility. On the other hand, the low solubility of ionic species can cause increased susceptibility of the structural materials to general corrosion and stress corrosion cracking (SCC).

There is a significant amount of operational experience with supercritical coal-fired power plants. In 2004, more than 460 units of coal-fired supercritical water power plants were in operation. However, there are significant differences between a nuclear reactor core and a fossil-fired boiler as summarized by Was et al. [2]. One key difference relates to the geometry and dimensions of critical components. A fossil-fired boiler consists of a large number of fire tubes that circulate water inside, with relatively thick walls (6-12 mm in thickness). In contrast, the core of a European SCW reactor [3] consists of 156 fuel assembly clusters, with the wall thickness of the fuel rod cladding being less than 1 mm, and the wall thickness of the water rods being approximately 0.5 mm. This implies much more stringent requirements for corrosion resistance in the core of a SCW reactor.

A second key difference is irradiation, affecting both the water chemistry and the alloy microstructure. Radiolysis can cause an increase of corrosion potential due to a higher rate of formation of oxygen and other oxidizing species such as H₂O₂, which can result in an increased susceptibility to SCC. The most challenging problem is the role of irradiation on the microstructure and how it affects degradation processes such as SCC. Irradiation assisted stress corrosion cracking (IASCC) is expected to be a generic issue on the basis of experiences in light water reactor installations.

This paper first briefly summarizes results of slow strain-rate tensile (SSRT) tests on various classes of alloys. Emphasis is then put on the SCC behavior of one of the candidate materials for several core components in the European design of the SCW reactor, with the aim identifying

and describing the specific failure mechanisms prevailing during SSRT tests in ultra-pure demineralized SCW.

2. Experimental

2.1 SSRT Tests

The paper was prepared with the following objectives:

- 1) Exploration of the mechanism of SCC for 316L stainless steel, in particular, in terms of the ratio of intergranular SCC (IGSCC), transgranular SCC (TGSCC) and ductile fracture of specimens loaded at different strain rates in an SCW environment.
- 2) Evaluation of the SCC susceptibility of AISI 316L, 316NG, 347H and Alloy 690 specimens loaded at the same strain rates in SCW environments.

Small tensile specimens (Figure 1) of commercially available AISI 316 L, 316 NG, 347 H and Alloy 690 were used for SSRT tests in ultra pure 550°C and 250 bar supercritical water solution with an electric conductivity of less than 0.1 $\mu\text{S}/\text{cm}$ at the autoclave inlet. The compositions of these alloys are provided in Table 1.

Material	C	Si	Mn	S	P	Cr	Ni	Fe	Others
316 L	<0.03	<0.75	<2.0	<0.03	<0.045	16-18	10-14	Bal.	Mo<3.0
316 NG	0.014	0.42	0.8	0.001	0.032	16.6	11.3	Bal.	Cu = 0.23 Mo = 2.11
347 H	0.048	0.29	1.84	0.013	0.026	17.58	10.7	Bal.	Nb = 0.56
Alloy 690	<0.04	<0.5	<0.5	<0.015		28-31	bal.	7-11	

Table 1 Chemical composition, in mass%, for the tested alloys.

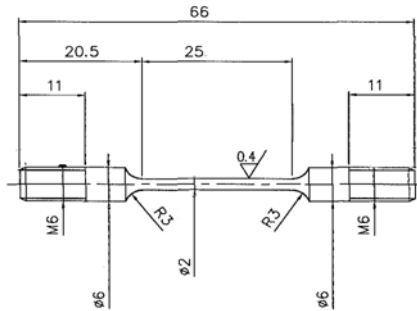


Figure 1 Schematic drawing of the tensile specimens for SSRT testing.

A flow chart of the test loop is shown in Figure 2. The system consists of a low-pressure part for the water chemistry control, and a high-pressure part incorporating an autoclave with a mechanical test rig. The chemical parameters such as pH, conductivity and dissolved oxygen concentration were measured continually in the low-pressure part of the loop, both at the inlet and the outlet from the high pressure part.

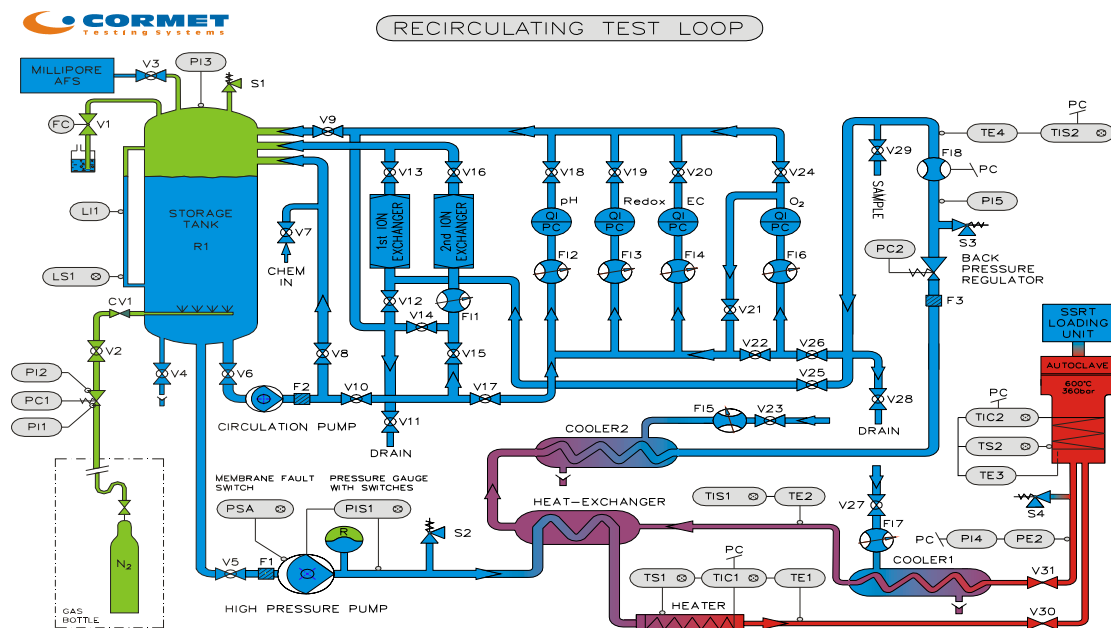


Figure 2 Flow chart of the SCW loop used for SSRT testing.

In this study, specimens were tested in the as-received condition, i.e. without additional heat treatment, except for the 316L-8 specimen, prior to exposure to the SCW environment. The specimens were first exposed at a constant pre-load 70 N (220 MPa) to SCW for 24h. Following

that, the specimens were strained at constant crosshead speed rate until failure. The autoclave was then cooled down as fast as possible (approximately 24 h) to avoid further oxide layer growth on the fracture surface.

2.2 Fractographic analysis

Fractographic analysis of failed specimens was carried out at the Department of Materials of the Faculty of Nuclear Sciences and Physical Engineering of Czech Technical University in Prague by means of a scanning electron microscope, Jeol JSM 840-A, in order to allow for the (i) identification of failure mechanisms taking place during SSRT tests, (ii) description of the influence of different test conditions (i.e. temperature, oxygen content and strain rate) on failure mechanism, (iii) evaluation of the ratio of SCC growth to ductile fracture on the failed specimen cross-sections.

The fractographic analysis required a cleaning of the fracture surfaces covered by oxide layers grown during the exposure in SCW. The cleaning procedure developed by the fractographic laboratory of the Department of Materials [4] consist of an ultrasonic cleaning in a solution recommended by ASTM Standard (HCl + hexamethylentetramin + water), followed by SEM observation to verify the efficiency of the cleaning. This procedure was applied in repetitive steps to avoid any unintentional alterations of the microfractography of the fractured surfaces.

3. Results and Discussion

3.1 Influence of strain rate for 316L SS

The first part of this study was published in the Journal of Nuclear Materials in 2010 [5]. The influence of SSRT test parameters on the occurrence of SCC was, in that paper [5], summarized on the basis of the fractographic results, showing the parameter regime where SCC is favored by high oxygen content and slow strain rate.

The present study summarizes results of further tests carried out in 2010 in JRC Petten. A summary of the loading parameters (i.e. applied nominal strain rates and maximal stress) and the

parameters of the SCW (i.e., temperature, pressure and oxygen content) as well as the main results of the SSRT tests is presented in Table 2. Stress-strain curves are shown in Figure 3.

Specimen	Temp. [°C]	Pressure [bar]	O ₂ [ppb]	Elongation rate** [μm/min]	Max. stress [MPa]	Time to fracture [s]	SCC area [%]
316L - 1	550	250	150	0.3	508	598 790	6.2
316L - 4				0.5	503	217 950	9.5
316L - 7				0.8	519	282 900	11.5
316L - 8*				1	389	359 403	2.4
316L - 6				1	434	197 222	0

*Heat treatment - 1020-1040 °C, 30 min., cooling in air

** Cross-head speed

Table 2 Summary of the test parameters and key results.

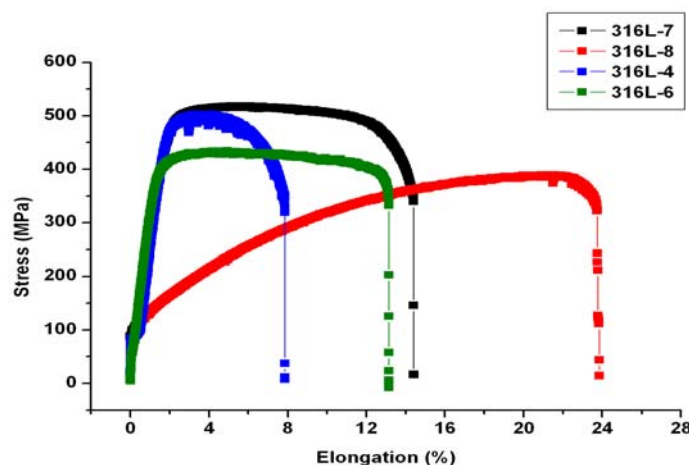


Figure 3 Stress-strain curves for 316L specimens tested at different strain rates (cf. Table 1).

Solution-annealed austenitic stainless steels normally exhibit significant strain hardening in 550 °C SCW. The absence of strain hardening, which is assumed to result from the prior work hardening, was already discussed in Novotny et al. [5] and Pentilla et al. [6]. Again the low degree of strain hardening observed in the SSRT test presented in this paper is assumed to result from cold work during manufacturing. The present 316L specimens showed similar behavior, therefore for specimen 316L-8 additional heat treatment (1020-1040 °C, 30 min., cooling in air)

was carried out, resulting in changes of mechanical properties: decrease of yield strength, values of upper tensile stress and a considerable increase of strain hardening. On the other hand, strain to failure significantly increased. These results are in line with the data measured by Pentilla et al. [6] for 316 NG stainless steel.

Fractographic analysis was carried out on 316L-1, 316L-4, 316L-7, 316L-6 and 316L-8 specimens tested at identical SCW conditions in order to evaluate the influence of strain rate and additional heat treatment. The main results of the SEM analysis of these specimens can be summarized as follows (see also Figures 4 and 5):

1) Failure of 316L-1, 316L-4, 316L-7 and 316L-8 specimens was initiated by transgranular stress corrosion cracks propagating from specimen surfaces. The length (depth) of these cracks did not exceed 300 μm , while the rest of the cross-sections failed by transgranular ductile fracture.

2) Several “secondary” stress corrosion cracks (in planes parallel to the fracture plane) were found on the surfaces of all analysed specimens. Was et al. [7, 8], however, used the crack depth and the crack density on the gage surface as an indicator of the IGSCC susceptibility. %IG requires significant crack growth to be observable. On the other hand, the significance of cracking on the gage surface is unknown and for cylindrical type of specimens (Figure 1) it is very difficult to make such analysis.

3) Change of the strain rate from 1 $\mu\text{m}/\text{min}$ to 0.8 $\mu\text{m}/\text{min}$ and to 0.5 $\mu\text{m}/\text{min}$, respectively, led to a change of the macroscopic morphology of the fracture surfaces. Number and length of stress corrosion cracks and measured size of fracture areas (from 0% for 316L-6 and 2.4% for 316L-8 to 9.5% for 316L-4, 11.5% for 316L-7 and 6,2% for 316L-1) increased with decreasing strain rate, with the exception of 316L-1.

4) Changes of strain rate have no significant influence on fracture micromorphology in areas corresponding to the SCC (micrographs in Figure 6a, b and c).

5) Heat Treatment (316L-8) had little effect on the fracture micromorphology compared to the 316L-6 specimen loaded by the same cross-head speed. Contrary to the 316L-6 specimens some indications of SCC were found on the fracture surface, but the SCC area was very small and , considering the specimen type used, these tests will have to be repeated.

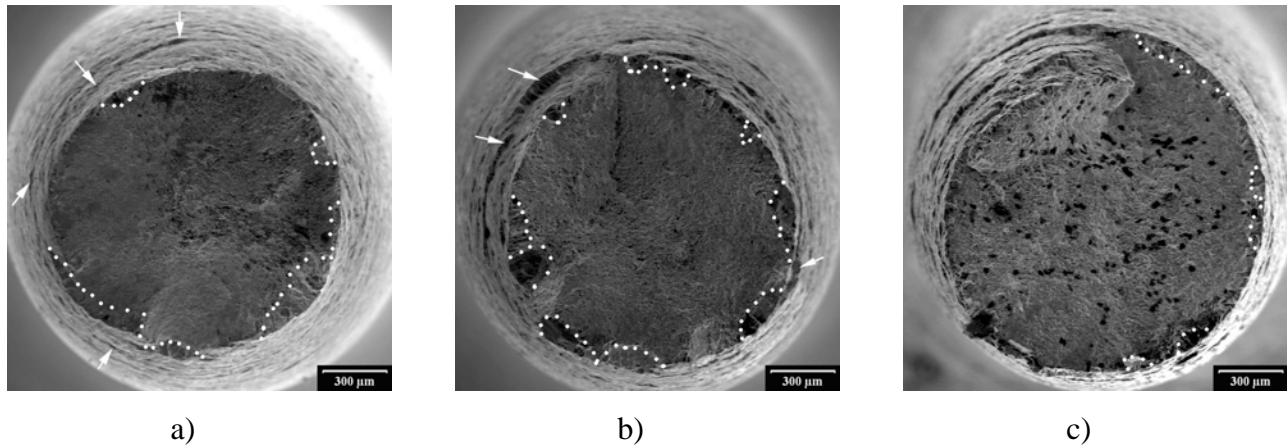


Figure 4 Fracture surfaces of specimens tested at different strain rates; a) 316L-4, b) 316L-7 and 316L-8. Areas exhibiting SCC features are marked by dotted lines (as received fracture surfaces).

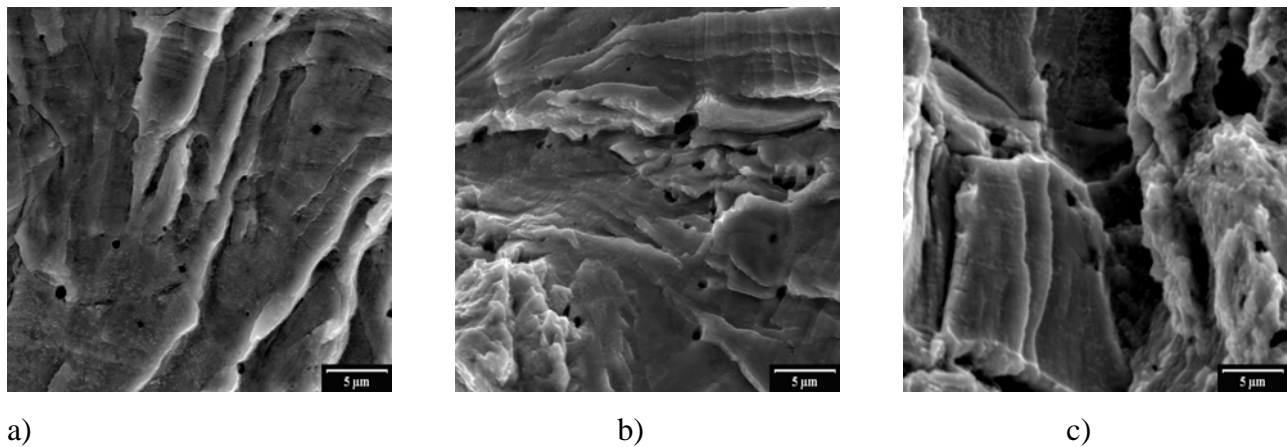


Figure 5 Influence of different strain rates on fracture surface micromorphology corresponding to SCC features (cleaned fracture surfaces); a) 316L-4, b) 316L-7 and c) 316L-8.

6) SCC features have not been detected on the fracture surface of Specimen 316L-6. The fracture morphology instead corresponds to final ductile rupture during the tensile test. Some

intergranular facets were sporadically observed in the central part of the fracture surface of Specimen 316L-6, but SEM analysis did not reveal any connection between these intergranular facets and the environmental attack from the specimen surface (Figure 6). Based on this finding we can assume that those intergranular facets did not result from corrosion processes.

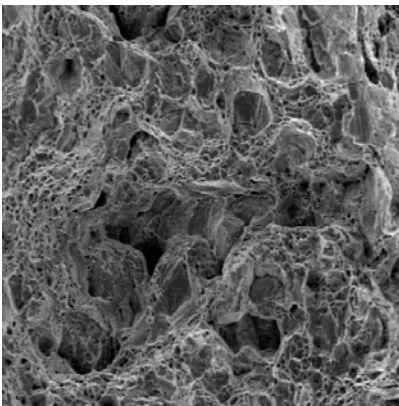


Figure 6 Facets of intergranular fracture surrounded by transgranular ductile dimples (316L-6 specimen with cleaned fracture surface).

In the present work, % IG SCC on the fracture surface was used as the evaluation criterion for SCC susceptibility. The presented results are in good agreement with those of Tsuchiya et. al. [9] measured for 304 and 316 stainless steels, whereas Tsuchya [9] did not find any %IG SCC on the fracture surface of 304 and 316 stainless steel specimens exposed at 550 °C SCW. It is a well-known fact that SCC susceptibility is increased by cold work and there are cases of failures of BWR components which have been attributed to heavy cold work of stainless steel with transgranular cracking initiated at the hardened surface and intergranular crack propagation into the soft part of the material [10]. This is in agreement with the results presented in this work, where the specimen surfaces were also affected by work hardening from the specimen machining (cf. absence of strain hardening in Figure 3), and SCC cracks always initiated transgranularly from the surface.

Fractographic analysis, however, can offer important and conclusive information about the mechanism of stress corrosion crack growth. The present fractographic findings confirmed that the proportion of SCC and ductile fracture on the fracture surfaces of specimens is governed by

the parameters of the SSRT tests, especially by the strain rate and the oxygen content. In Figure 7, the influence of SSRT test parameters on the occurrence of SCC is summarised on the basis of the present fractographic results, showing the parameter regime where SCC is favoured by high oxygen content and slow strain rate.

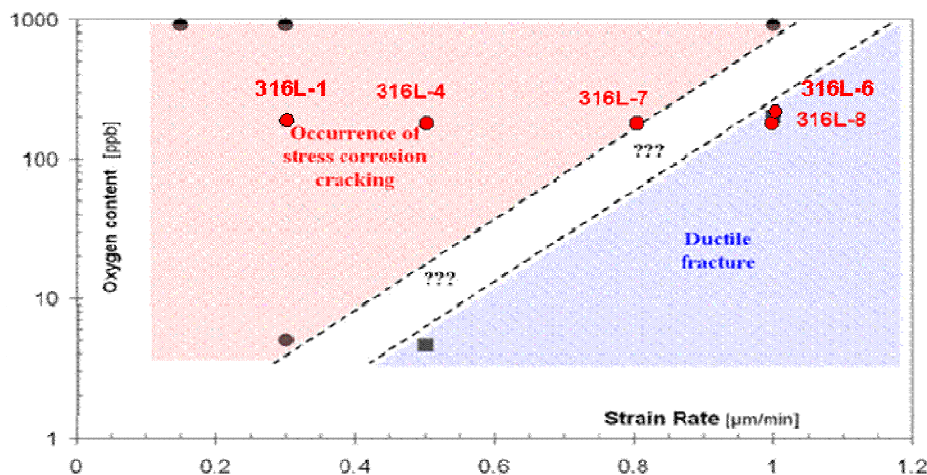


Figure 7 Map delineating the occurrence of TGSCC in 550 °C SCW environment for different strain rates and oxygen contents. (The data marked by black dots were measured and published by Novotny et al. [5] in 2010.)

Future experiments are planned to show to what extent the presented SCC regime of 316L stainless steels can be used for an extrapolation of the stress corrosion behaviour to conditions different from the present ones.

3.2 SCC susceptibility of AISI 316L, 316NG, 347H and Alloy 690 specimens

A summary of the loading parameters (i.e. applied nominal strain rates and maximal stress) and the parameters of the SCW (i.e., temperature, pressure and oxygen content) as well as the main results of SSRT tests for four different materials, AISI 316 L, 316 NG, 347 H and Alloy 690, is presented in Table 3.

Specimen		Temp. [°C]	Pressure [bar]	O ₂ [ppb]	Elongation rate* [µm/min]	Max. stress [MPa]	Time to fracture [s]
Material	Label						
316L	316L - 1	550	250	150	0.3	506	598 790
316NG	6 - 1				0.3	351.9	157 6000
347H	7 - 1				0.3	442.6	924 095
Alloy 690	A - 1				0.3	440.4	1 712 330

* Cross-head speed

Table 3 Summary of the test parameters and key results.

Stress-strain curves of specimens listed in Table 1 are given in Figure 8.

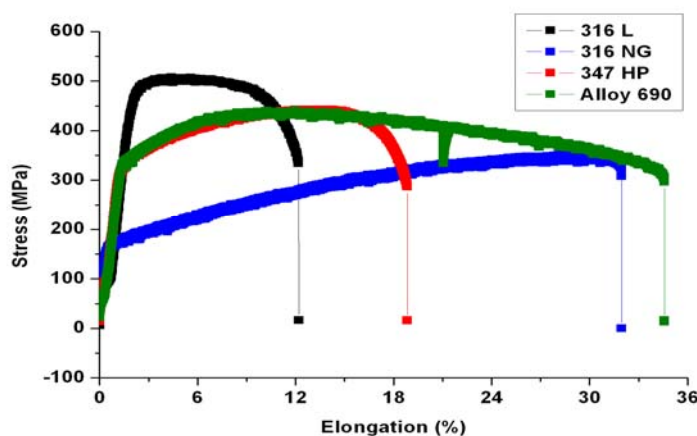


Figure 8 Stress-strain curves for 316L, 316NG, 347H and Alloy 690 specimens tested at different strain rates (cf. Table 2).

It was thought that Specimen 316 NG failed during the test since a decrease of stress to zero was recorded by our data acquisition system (see Figure 8). Surprisingly, the specimen was found unbroken after the autoclave was opened therefore this specimen was ruptured in the fractographic laboratory. Subsequent SEM analysis did not reveal the reason why that happened. Typically 316 NG and 347 H austenitic stainless steels exhibited strain hardening in contrast to the heavily work hardened 316 L specimen (see also the result in Figure 8). These results are in

agreement with data measured by Pentilla et al [6]. The yield stress, maximum stress and strain hardening capacities of 347 H and Alloy 690 are similar. On the other hand the 347 H specimen failed at much lower elongation than Alloy 690. The gradual decrease of stress for the Alloy 690 specimen resulted from the onset of necking until the specimen failed.

Fractographic analysis was carried out of the specimens from the three different materials tested under identical parameters of the SCW (temperature, pressure and oxygen content) and with the same strain rates (see Table 2) and compared to the results of the 316L specimen exposed in the same SCW and loaded by the same cross-head speed published in Novotny et al. [5]. The results of the SEM analysis are given in Figures 9 and 10.

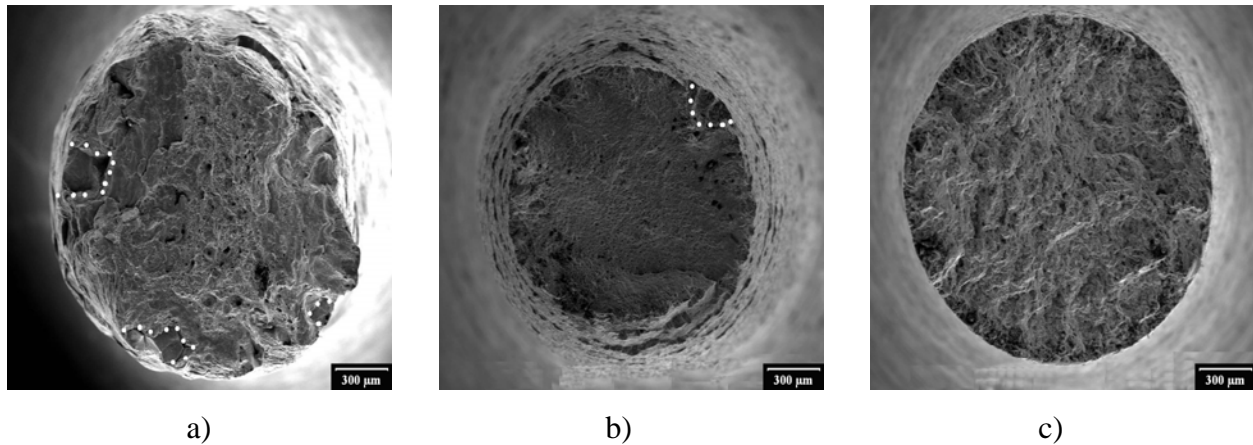


Figure 9 Fracture surfaces of specimens tested under the conditions described in Table 2; a) 316 NG, b) 347H and c) Alloy 690. Areas exhibiting SCC features are marked by dotted lines (as received fracture surfaces).

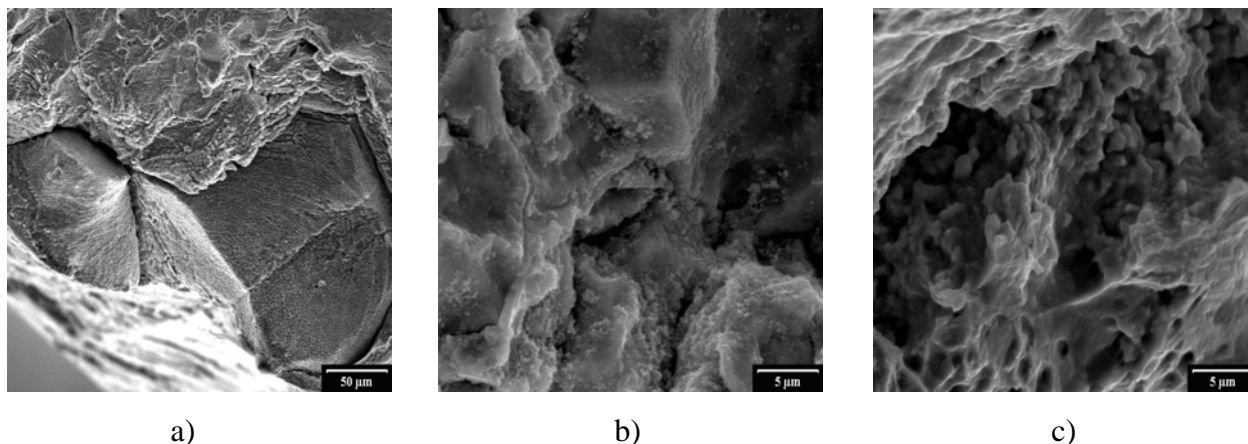


Figure 10 Fracture surface micromorphology corresponding to SCC features (cleaned fracture surfaces); a) 316 NG, b) 347 H and c) Alloy 690.

The results of the fractographic analysis were summarized as follows:

- The efficiency of cleaning method used was relatively low, especially for 347 H and Alloy 690 specimens (see Figure 10).
- Sporadic intergranular facets connected to the surface of the specimen were observed on fracture surfaces of the 316 NG and 347 H specimens.
- The Alloy 690 specimen failed by ductile fracture.

The results presented document the highest corrosion resistance of Alloy 690, among these four materials exposed at the same elongation rate to the selected SCW environment. Nevertheless, the corrosion resistance of austenitic stainless steels 316NG and 347H is significantly higher than the corrosion resistance of cold worked AISI 316L. Higher yield stress (350 MPa) and considerably lower resistance to fracture for 347 H compared to the results of Pentilla et al. [6] (yield stress was approximately 250 MPa) was again probably caused by cold work developed during the manufacturing process. Initiation of intergranular SCC found at the fracture surfaces of 316 NG and 347H will probably be strongly influenced by the grain size. The presented results indicate that steels with coarser grains show higher corrosion resistance. This conclusion will be tested in the next series of experiments, since in the case of the steels studied the change of corrosion resistance could be also influenced by different chemical composition.

4. Conclusions

The present paper is a continuation of a systematic analysis of the effect of strain rate and other parameters on SCC of AISI 316L, in an attempt to identify and describe failure processes prevailing during SSRT tests in demineralised SCW solution with controlled water chemistry. The main findings can be formulated as follows:

- the SCC resistance of austenitic stainless steel 316L in ultrapure SCW seems satisfactory based on the results obtained from SSRT tests, in particular if one notes that the specimens had undergone some work hardening during the manufacturing process. Even at the lowest strain rate, a serious increase of SCC susceptibility, as typically characterized by IGSCC crack growth, was not observed.
- The failure process prevailing during SSRT testing is caused by a combined influence of environment and external loading. SSRT tests are therefore difficult to interpret and a detailed understanding of the influence of individual test parameters will necessitate more extensive sets of test data.
- Fractographic analysis of failed specimens has confirmed that the proportion of SCC and ductile fracture in the failure process of individual specimens is affected by the parameters of the SSRT tests, especially the strain rate and the oxygen content.
- Based on fractographic findings a phenomenological map describing the SCC regime of SSRT test parameters is proposed for AISI 316L.
- The fracture resistance of 316L in 550°C SCW was the lowest of all four tested materials, on the other hand, the occurrence of the IGSCC initiation sites on the fracture surfaces of 316NG and 347H specimens presents evidence inconsistent with the data from 316 L.
- The need for further pre-normative research into harmonised SSRT test procedures for SCC susceptibility assessment has been pointed out, in particular, with regards to the effect of cold working associated with specimen machining.

5. References:

- [1] D. Bittermann, D. Squarer, T. Schulenberg, Y. Oka, Economic Prospects of the HPLWR, GENES4/ ANP2003, Kyoto, Japan, September 15-19 (2003), Paper 1003.
- [2] G.S. Was, P. Ampornrat, G. Gupta, S. Teysseyre, E.A. West, T.R. Allen, K. Sridharan, L. Tan, Y. Chen, X. Ren, C. Pister, Corrosion and Stress Corrosion Cracking in Supercritical Water, *Journal of Nuclear Materials*, 371 (2007) 176–201.
- [3] C. Koehly, T. Schulenberg, J. Starflinger, HPLWR Reactor Design Concept, 4th International Symposium on Supercritical Water-Cooled Reactors, Heidelberg, Germany, March 8-11 (2009), Paper 37.
- [4] J. Siegl, P. Haušild, Fractographic Analysis of Specimens Failed in Slow Strain Rate Tests, Faculty of Nuclear Sciences and Physical Engineering, Czech Technical University, Report Number: V-KMAT-758/09, Prague, Czech Republic (2009).
- [5] R. Novotny, P. Hähner, J. Siegl, P. Haušild, S. Ripplinger, S. Penttilä and A. Toivonen, Stress Corrosion Cracking Susceptibility of Austenitic Stainless Steels in Supercritical Water Conditions, *Journal of Nuclear Materials*, Article in Press
- [6] S. Penttilä, A. Toivonen, L. Heikinheimo, R. Novotny, Corrosion Studies of Candidate Materials for European HPLWR, ICAPP '08, Anaheim, California, USA, June 8 – 12 (2008).
- [7] G. S. Was and S. Teysseyre, “Challenges and Recent Progress in Corrosion and Stress Corrosion Cracking of Alloys for Supercritical Water Reactor Core Components,” Proceedings of the 12th International Conference on the Environmental Degradation of Materials in Nuclear Power Systems – Water Reactors, American Nuclear Society, 1343-1357, Salt Lake City, UT, August 14-18, 2005.
- [8] G. S. Was, S. Teysseyre, and J. McKinley, “Corrosion and Stress Corrosion Cracking of Iron and Nickel-base Austenitic Alloys in Supercritical Water,” Proc. NACE Annual Conference, Corrosion 2004, paper #04492, New Orleans, LA (2004).
- [9] Y. Tsuchiya, F. Kano, N. Saito, A. Shioiri, S. Kasahara, K. Moriya, H. Takahashi, SCC and Irradiation Properties of Metals under Supercritical-water Cooled Power Reactor Conditions GENES4/ANP2003, Kyoto, Japan, September (2003) , Paper 1096.
- [10] M. Tsubota, Y. Katayama, Y. Kanazawa, Relation Between the Mechanical Properties and SCC Behavior of the Alloys Used in High Temperature Water, 13th International Conference on

Environmental Degradation of Materials in Nuclear Power Systems, Whistler, British Columbia,
Canada August 19 – 23 (2007).